

Beamforming for Blind Surveys at the ATA

G. R. Harp

8/6/3, revised 9/11/03

Abstract

The ATA is designed to simultaneously operate in two data collection modes using 1) an imaging correlator and 2) 16 independently steerable phased array beamformers. One or more of these beamformers may be dedicated to a “blind” survey for relatively high power continuous or transient sources. One proposal is to raster an ordinary phased array beam across the primary FOV of the antenna to generate snapshot images of the sky. We offer an alternative approach that is advantageous for discovery of strong non-continuous sources and, depending on search conditions, is significantly advantageous for the discovery of continuous sources. This approach is similar to utilization of a beam taper, where some synthetic beam gain is sacrificed in exchange for wider solid angle coverage. Instead we propose a complex-tapering scheme that gives a large solid angle but with less degradation of beam gain.

Introduction

The 16, independently-steerable phased array beams provided by the ATA IF Processor will allow numerous, simultaneous observations in the broad field of view (FOV) of the ATA primary beam. At least 3 of these beams will be dedicated to a targeted ETI search, which forms narrow beams on a prepared list of candidate stars. These stars are chosen for a perceived high probability of supporting life. The remaining 13 beams will be applied for a variety of purposes, such as pulsar timing or a blind survey for unknown strong or transient sources. This paper focuses on optimization of the blind survey.

Conceptually, the blind survey is performed by rastering one ATA beam rapidly across the antenna FOV. Because this is a piggyback observation mode, the antenna pointing and observation duration is set by another process, such as the radio-astronomical observing program. The raster is timed such that it fits conveniently within the scheduled time period for a single RA-Dec pointing of the array.

The blind survey gives us the chance to hedge our bets w.r.t. the targeted ETI search. In case we guess wrongly about which stars to observe, the blind survey will eventually provide continuous solid-angle coverage of a large fraction of the sky, albeit at a lower sensitivity. The blind survey also searches for strong but intermittent ETI sources. While an ETI transmitter may be on our targeted search list, if it is not turned on for the short period when we observe it then it won't be detected. The blind survey returns to the same sky point multiple times during the lifetime of the ATA, thus giving us greater opportunity to catch intermittent transmitters. Finally, the blind survey will reveal new astronomical transient sources and thus serves a third purpose.

This paper discusses beamforming techniques that optimize the blind survey. Instead of rastering a simple beam, we propose to raster a large solid angle beam. The proposed beam is formed using a complex tapering scheme that increases sensitivity to strong

intermittent sources without sacrificing sensitivity to weak continuous sources – as is the case for beams generated with a simple “real” taper.

Sensitivity to Continuous or Intermittent Sources

To make comparisons between beamforming approaches, we distinguish between two types of search product: (1) discoveries of continuous ETI transmitters, (2) discoveries of intermittent ETI transmitters. We firstly derive the sensitivity to continuous sources.¹ For simplicity we shall assume that our SETI detector bandwidth is larger than the bandwidth of the arriving signal. In this case the rms uncertainty in the noise power seen by our detector after an integration time τ is given by the radiometer equation

$$\Delta P = \frac{P_N}{\sqrt{N_{\text{Samples}}}} = \frac{k_B T_s \beta}{\sqrt{\beta \tau}} = \frac{k_B T_s \sqrt{\beta \tau}}{\tau}, \quad (1)$$

where P_N is the noise power, N_{Samples} is the number of independent samples, T_s is the system temperature, k_B is Boltzmann’s constant, and β is the frequency bandwidth of a single bin in the post-FFT analyzed signal. Assuming a point source transmitter with EIRP of P_v , the received power from a source at distance r is

$$P_r = \frac{1}{2} (G_b A_d) \frac{P_v}{4\pi r^2}, \quad (2)$$

where A_d is the effective area of a single dish and G_b is the synthetic beam gain (for example, with 32 dishes and uniform weighting $G_b = 32$). We assume the receiver measures only a single polarization, hence the factor of $1/2$. The signal to noise ratio is then

$$\frac{P_r}{\Delta P} = \frac{G_b A_d P_v \sqrt{\tau}}{8\pi r^2 k_B T_s \sqrt{\beta}}. \quad (3)$$

To qualify as a detection, $P_r/\Delta P$ must exceed some fixed level, m . We can then use this equation to solve for r_{max} , the maximum distance at which the transmitter may be detected.

$$r_{\text{max}} = \sqrt{\frac{G_b A_d P_v \sqrt{\tau}}{8\pi m k_B T_s \sqrt{\beta}}}. \quad (4)$$

Because this is a piggyback measurement, we are given a fixed time period T while all the antennas illuminate a given sky patch, after which they move on. We wish to achieve approximately uniform sensitivity over the antenna primary beam solid angle Ω_p . Thus,

¹ This discussion follows a similar one in “SETI 2020: A Roadmap for the Search for Extraterrestrial Intelligence,” Eds. R. D. Ekers et al., SETI Press, 2002, p. 444.

$$\tau = T \Omega_b / \Omega_p . \quad (5)$$

where Ω_b is the synthetic beam solid angle.² Finally, the *a priori* detection probability for a continuous source, P_C , is proportional to the total volume of space probed³. Since we are covering the entire primary beam this is

$$P_C \propto \frac{\Omega_p}{3} r_{\max}^3 \propto \Omega_b^{\frac{3}{4}} G_b^{\frac{3}{2}}, \quad (6)$$

and we have suppressed quantities we aren't interested in.

Coherent Integration

Until now we have assumed incoherent signal integration – i.e. the coherent integration time (length of FFT) is smaller than τ . This is not always the case. For example, if only 5 minutes were devoted to a single antenna pointing / IF tuning, then each synthetic beam pointing is given only 0.02 seconds of integration time (FFT bin width of 45 Hz). Since we are capable of 1 second integrations using the current SETI detector, we must consider how the signal to noise ratio is affected in the coherent integration regime.

When the coherent integration time is increased, the bandwidth of each frequency bin (after FFT) is decreased in proportion to τ , reducing the observed noise power in each bin. Replacing β with $1/\tau$ in Eq. 1 leads to

$$P_{C,Coh} \propto \Omega_b^{\frac{3}{2}} G_b^{\frac{3}{2}} . \quad (7)$$

Intermittent Sources

For an intermittent source, the signal must exceed our detection threshold so the *a priori* probability of detection P_I is proportional to P_C . But the source must also be turned on, so P_I contains an additional factor of τ , leading to

$$P_I \propto \Omega_b^{\frac{7}{4}} G_b^{\frac{3}{2}} \quad (8)$$

for incoherent integration or

$$P_{I,Coh} \propto \Omega_b^{\frac{5}{2}} G_b^{\frac{3}{2}} \quad (9)$$

for coherent integration.

² A more precise definition of Ω_b is the solid angle over which the synthetic beam has gain greater than 50% of its maximum value.

³ This assumes a constant transmitter density over the probed region of the galaxy.

Comparison of Ordinary and Simple-Taper Beams

Before demonstrating complex-taper solutions, we consider a simple-taper beam. An ordinary beam uses signal delays to form a single maximum on the sky and gives every antenna unit weight. A tapered beam gives reduced weight to antennas at the periphery of the array. The benefit of the tapered beam is that it covers a larger area of the sky at all times, giving it greater sensitivity to intermittent sources.

As a simple example, consider a 128×128 array of antennas laid out on a square grid as indicated by the white square on the left hand side of Fig. 1. The left hand side of Fig. 2 shows the beam pattern for this array. We choose gain and angular scales such that $\Omega_b = G_b = 1$ for this beam.

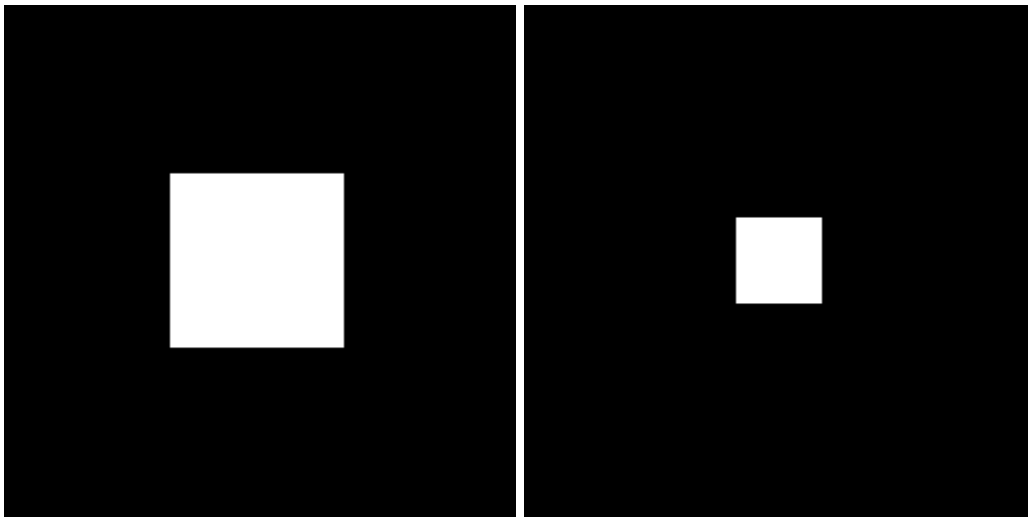


Figure 1: **Left:** depiction of antenna layout for a square array (white square) comprising 128×128 antennas. **Right:** A crude taper is applied where only the central quarter of the antennas have nonzero weight in the beam.

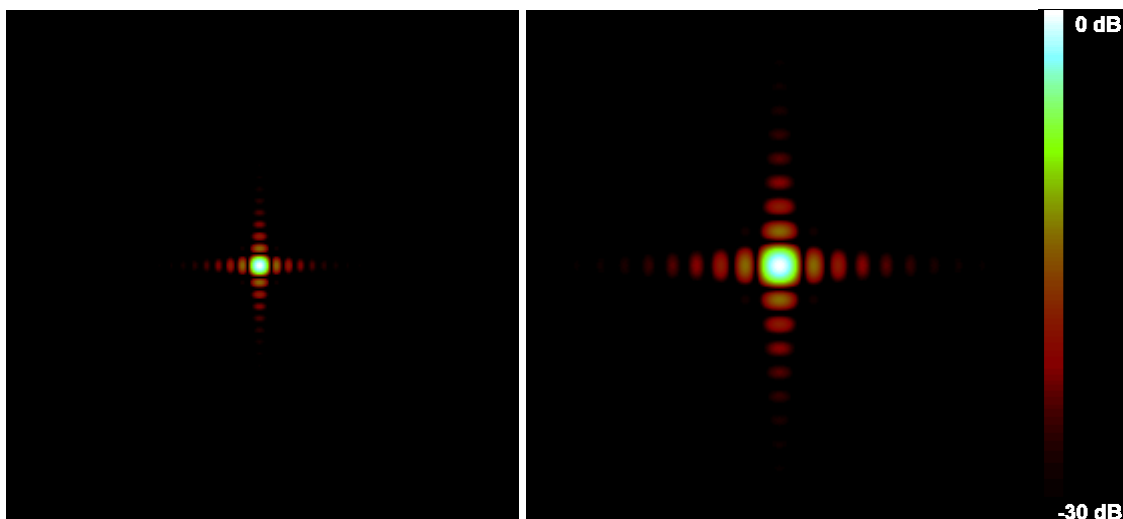


Figure 2: The beam patterns of the antenna arrays depicted in Fig. 1. **Left:** Pattern of 128×128 square array. **Right:** Pattern of tapered beam.

On the right hand side of Fig. 1, we demonstrate a taper by giving $\frac{3}{4}$ of the antennas zero weight, retaining only the inner $\frac{1}{4}$ of the antennas. The beam pattern for this tapered array is shown on the right in Fig. 2. Evidently, Ω_b of the tapered beam is 4 times as large as that of the original beam.

Not evident in Fig. 2 is the relative gains of the two beams; the tapered gain is $\frac{1}{4}$ that of the original beam. From this we can work out P_C and P_I for the two beams as in Table 1. For incoherent integration, the tapered beam shows improvement for P_I but a loss of sensitivity for P_C . For coherent integration however, $P_{C,Coh}$ is unchanged. Including the improvement in $P_{I,Coh}$, one can conclude that we should dispose of all the antennas but one. If the antenna had isotropic gain, this would be the case⁴. We shall see below how directional antennas leads to an optimum when $\Omega_b = \Omega_p$.

Table 1: Compilation of the probabilities of detecting continuous ETI transmitters (P_C) and intermittent ETI transmitters (P_I) for various beams described in the text.

Beam Name	Ω_b	G_b	P_C	$P_{C,Coh}$	P_I	$P_{I,Coh}$
Ordinary Square	1	1	1.0	1.0	1.0	1.0
Tapered Square	4	$\frac{1}{4}$	0.35	1.0	1.41	4.0
Four Square Beam	16	$\frac{1}{4}$	1.0	8.0	16.0	128.0

Four Square Beam

The tapered beam is not optimal because not all antennas contribute, so consider the following. If we divide the original array into four equal, square sub-arrays, we find that each sub-array has the tapered beam pattern. If these beams are all pointed at the same sky patch, there is no way to prevent them from interfering with one another to form the ordinary beam. The trick is to point each sub-array towards a *different* sky patch. This is demonstrated in Fig. 3.

⁴ This analysis does not take into account practical issues such as: 1) it is difficult to integrate for long times as this corresponds to a very long FFT, 2) because of interstellar scintillation, it makes no sense to have an FFT bin width less than 0.01 Hz or coherent integration time of 100 s (see reference in footnote 1).

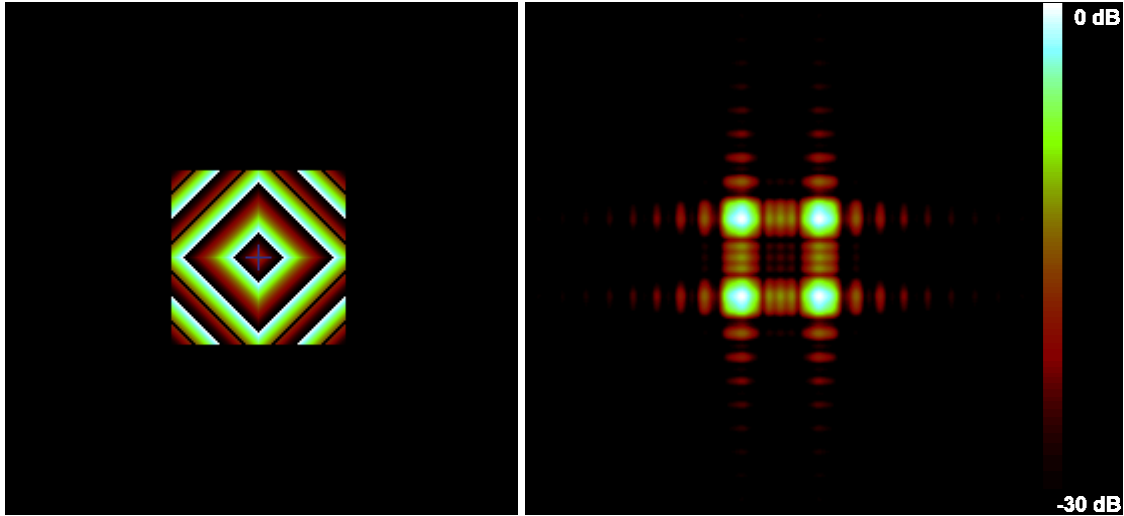


Figure 3: **Left:** The square array of Fig. 1 is modified by applying a variable phase to the signal from each antenna. Here we represent the phase as it varies from $-\pi$ (black) to π (white). The amplitude of each antenna signal is unity. **Right:** The beam pattern of this array. The strongest features are four maxima, each of which look like the tapered beam of Fig. 2.

In Fig. 3, each antenna is given unit weight, but a variable phase points the sub-arrays in different directions. The resulting beam is the superposition of four tapered beams with each one sampling a different patch of sky. A side by side comparison of line scans through the tapered beam and four-square beam is shown in Fig. 4. Like the tapered beam, $G_b = 1/4$, but now $\Omega_b = 16$. P_C and P_I for this “four square” beam are displayed in Table 1 and show substantial improvement compared to the tapered beam.

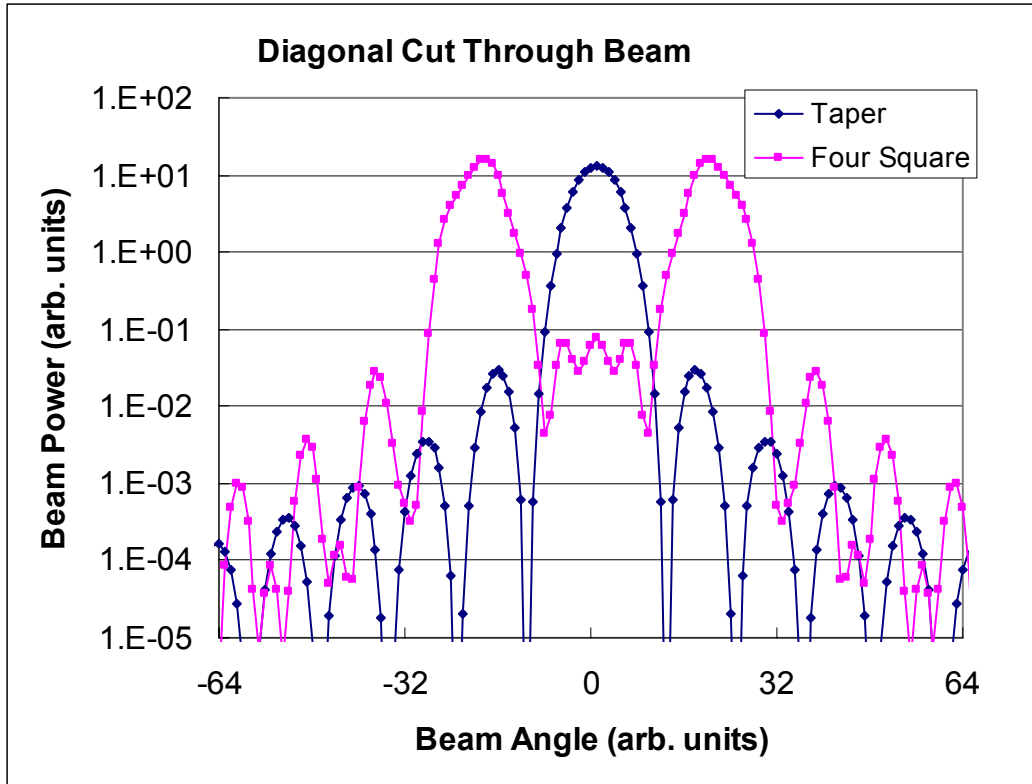


Fig. 4: Diagonal line scans through the tapered beam of Fig. 2 (right) and the four square beam of Fig. 3 (right). The peaks of the four square beam have approximately the same peak gain and approximately the same width as the peak of the tapered beam.

For incoherent integration, the four square beam has the same sensitivity to continuous ETI sources as the ordinary beam, but is 16 times more sensitive to intermittent sources. This is already a strong argument in favor of the four square beam. For coherent integration the argument is even stronger since the four square is 8 or 128 times more sensitive to continuous or intermittent sources, respectively. Because we foresee situations where coherent integration applies, these results are quite encouraging.

What we have sacrificed to obtain such improvements is direction information. If we raster the four square beam across our FOV, the image we obtain would be quite poor. However, the correlator will be generating a high quality image of the FOV anyway, so perhaps there is no need for image quality in the blind survey. In this case, it might be better to use something like the four square beam.

Complex Tapered Beams

As a final example, we extend the concept of the four square beam to a continuous range of pointing directions. Suppose that we break our original array into 16 square sub-arrays. Each sub-array will produce a beam that is 16 times as large as the original, but having $G_b = 1/16$. To point each beam in a different direction, we must increase the phase *slope* applied to each sub-array as the distance, ρ , of that sub-array from the array center increases. That is

$$\text{phase slope} \equiv \frac{d\phi}{dr} \propto \rho.$$

To extend this result to the continuous case, we treat ρ as a continuous variable and integrate to obtain the phase as a function of radius, $\phi \propto \rho^2$. This is what we call a complex taper⁵. It can be regarded as applying a spatial chirp to the antenna signals. Just as the Fourier transform of a chirp has power over a continuous range of frequencies; the beam of a chirped antenna pattern has power over a continuous range of angles. One example is shown in Fig. 4.

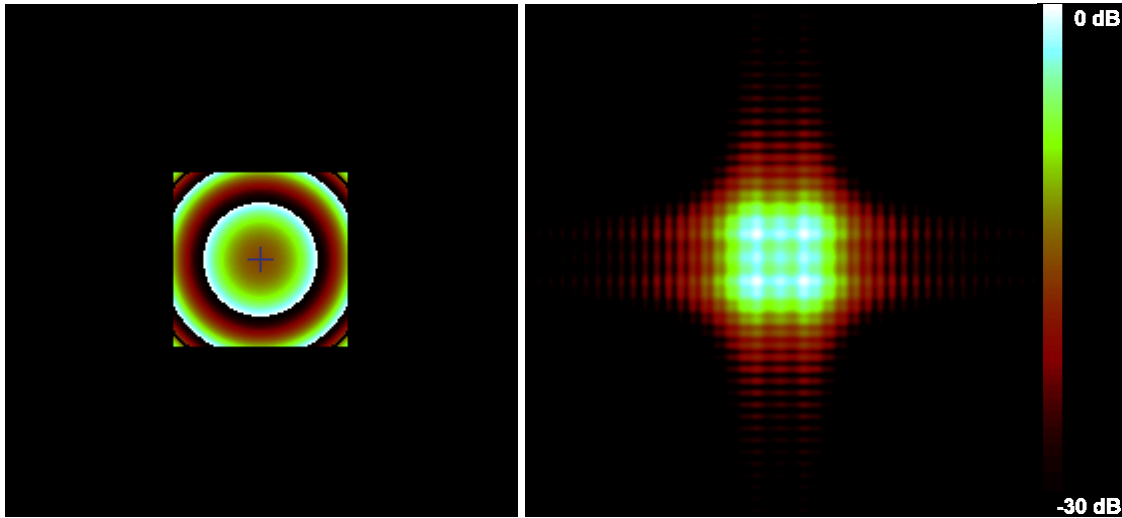


Figure 4: **Left:** The phase of the coefficient applied to each antenna in the complex tapered beam. The angular scale is the same as in Fig. 3. **Right:** The complex tapered beam pattern.

In Fig. 4 we have chosen a strong chirp, leading to a very broad beam pattern. Ω_b is about 100 times as large as the original beam, hence G_b must be approximately 0.01. This fractional increase of Ω_b is roughly what would be necessary to optimize the synthetic beam pattern at the ATA (see below). Although this figure demonstrates the basic idea of the complex tapering, the method has not been optimized. The beam amplitude variations present on the right hand side of Fig. 4 are large and could be improved by optimizing the chirp shape or amplitude.

But this square grid is not a realistic approximation of the ATA. The next obvious step is to apply complex tapers in simulations of real ATA beams based on the proposed ATA antenna layout. Such a study has begun, and promising results are obtained. The chirped

⁵ Mathematically, a spatial chirp has the form of a complex Gaussian: $\exp\left(-i\frac{r^2}{\alpha^2}\right)$. Just as with an

ordinary Gaussian, the Fourier transform of this function is another complex Gaussian, so we can immediately deduce the shape of the resultant beam pattern.

ATA beams are not as clean as the ones shown here, but otherwise have a similar character. Because the ATA antenna density is not constant across the array, obvious optimizations (i.e. different functions for $\phi(\rho)$) suggest themselves. Nevertheless, we end our presentation for now. If the ideas presented here generate sufficient interest, we shall pursue realistic simulations and optimizations for the ATA.

Optimizing the Synthetic Beam Width

A naïve extrapolation of these ideas suggests that the wider your synthetic beam, the better it is for ETI searches. But there is a limit. The synthetic beam pattern of an array with only one antenna is isotropic. Such an array looks for signals arriving from all directions. But the ATA antennas have significant gain only over the primary beam width, hence it is not possible to increase the effective value of Ω_b beyond Ω_p . Apart from this factor, detection probability increases with increasing Ω_b , so we conclude that the optimum occurs for $\Omega_b \sim \Omega_p$.

Conclusion

We find that the optimal synthetic beam solid angle for blind survey is on the order of the antenna primary beam solid angle. We describe a method (complex taper) for achieving large solid angle beams while maintaining relatively large synthetic beam gain. A beam pattern of this type should be considered for blind surveys at the ATA.

Acknowledgement

The author gratefully acknowledges Mike Davis for critical reading and suggestions throughout this memo's development. Although he is not to blame for any errors that may exist in this paper, there would certainly be many more without his help.